View metadata, citation and similar papers at core.ac.uk

brought to you by CORE

provided by Repositorio da Producao Cientifica e Intelectual da Unicamp

AIP | Journal of Mathematical Physics

# The interaction of outgoing and ingoing spherically symmetric null fluids

Paulo R. Holvorcem, Patricio S. Letelier, and Anzhong Wang

Citation: Journal of Mathematical Physics **36**, 3663 (1995); doi: 10.1063/1.530989

View online: http://dx.doi.org/10.1063/1.530989

View Table of Contents: http://scitation.aip.org/content/aip/journal/jmp/36/7?ver=pdfcov

Published by the AIP Publishing

**Articles you may be interested in**

Microphase separations of the fluids with spherically symmetric competing interactions
J. Chem. Phys. **137**, 114703 (2012); 10.1063/1.4754022

Ingoing and outgoing waves in time-domain simulation of wind instruments
J. Acoust. Soc. Am. **120**, 3332 (2006); 10.1121/1.4781269

Junction conditions on null hypersurfaces for spherically symmetric metrics
J. Math. Phys. **32**, 1537 (1991); 10.1063/1.529262

On the gravitational interaction of plane symmetric clouds of null dust
J. Math. Phys. **32**, 1017 (1991); 10.1063/1.529377

On spherically symmetric perfect fluid solutions
J. Math. Phys. **26**, 771 (1985); 10.1063/1.526565

Did your publisher get
18 MILLION DOWNLOADS in 2014?
AIP Publishing did.

AIP Publishing

THERE'S POWER IN NUMBERS. Reach the world with AIP Publishing.

This article is copyrighted as indicated in the article. Reuse of AIP content is subject to the terms at: http://scitation.aip.org/termsconditions.

Downloaded to IP: 143.106.108.182 On: Mon, 22 Jun 2015 16:58:31

# The interaction of outgoing and ingoing spherically symmetric null fluids

Paulo R. Holvorcem[a)]
*Center for Relativity, University of Texas at Austin, Austin, Texas, 78712-1081*

Patricio S. Letelier[b)]
*Isaac Newton Institute for Mathematical Sciences, Clarkson Road, Cambridge, United Kingdom*

Anzhong Wang[c)]
*Departamento de Astrofísica, Observatório Nacional-CNPq, Rua General José Cristino, 77, Rio de Janeiro, RJ, Brazil 20921*

(Received 1 December 1994; accepted for publication 1 March 1995)

Using similarity methods, the Einstein field equations coupled to two oppositely directed null fluids for a spherically symmetric space–time are reduced to an autonomous system of three ordinary differential equations. The space of solutions is studied in some detail and solutions are found that represent: (i) the backscattering of an initially outgoing thick null fluid shell in a background gravitational field with a central naked singularity, (ii) the formation of strong space–time singularities by the interaction of thick null fluid shells, (iii) the interaction of a core of null radiation with an incoming shell of null fluid, and (iv) cosmological models of Kantowski–Sachs type with initial and final singularities clothed by apparent horizons. © *1995 American Institute of Physics.*

## I. INTRODUCTION

Null fluid models are a good representation of a flux of massless particles such as photons of different energies and massless neutrinos. We can think of a spherical body, say, a star, that emits bursts of massless particles mainly along the radial direction. Since the mass (energy) curves the space–time, we have that the space–time curvature acts as a nontrivial index of refraction producing partial reflection of the radiation.[1] Then associated with an outgoing flux of radiation we will also have an ingoing one. The intensity of this last flux may be small compare with the first, but it may produce dramatic effects due to the nonlinearity of the Einstein equations. Also, a flux of ultrarelativistic particles can be approximated by a null fluid; even the gravitational radiation itself in certain limits has been thought of in the same way.

There are simple exact solutions of the Einstein equations in which a small amount of backscattered radiation is enough to produce strong singularities of the space–time by mutual focusing of the energy.[2,3] Also, the interaction of null fluids is one of the principal ingredients of the mass inflation phenomenon.[4] In this case the dynamics of a black hole is modeled by a Reissner–Nordstrom solution (whose causal structure is similar to that of the Kerr solution) and two interacting null fluids traveling in opposite radial directions. For simplicity, the interaction of the null fluids is studied in a fixed Reissner–Nordstrom geometry.

The actual solving of the Einstein equation coupled to null fluids traveling in opposite directions for a spherically symmetric space–time is not an easy task, amounting to solving a nonlinear system of coupled partial differential equations. The search for the general exact solution of this

[a)]Electronic mail: paulo@schild.ph.utexas.edu
[b)]Permanent address: Departamento de Matemática Aplicada, Instituto de Matemática, Estatística e Ciência da Computação, Universidade Estadual de Campinas, Campinas, SP, Brazil 13081-970; electronic mail: letelier@ime.unicamp.br
[c)]Electronic mail: wang@obsn.on.br

0022-2488/95/36(7)/3663/13/$6.00

© 1995 American Institute of Physics

This article is copyrighted as indicated in the article. Reuse of AIP content is subject to the terms at: http://scitation.aip.org/termsconditions. Downloaded to IP: 143.106.108.182 On: Mon, 22 Jun 2015 16:58:31

system is hopeless. Even more, meaningful particular exact solutions are not known. An alternative approach is to look for Lie symmetries that allow its reduction to a system of ordinary differential equations. This last approach is the subject of the present article.

The reduction of the problem to the study of a system of ordinary differential equations allows us to find solutions that describe: (a) the backscattering of an initially outgoing null fluid shell in a background gravitational field with a central naked singularity, (b) the formation of strong space–time singularities by the interaction of null fluid shells, (c) the interaction of a core of null radiation with an incoming shell of null fluid, and (d) cosmological models of Kantowski–Sachs type[5] with initial and final singularities clothed by apparent horizons.[6]

In Sec. II, we present the Einstein field equations coupled with ingoing and outgoing null fluids for a spherically symmetric space–time, and make use of a Lie point symmetry to reduce them to an autonomous system of three ordinary differential equations; in Sec. III we study this autonomous system in some detail. In Sec. IV we interpret the different classes of solutions, and in Sec. V we conclude by discussing the significance and limitations of the solutions found in this article.

## II. FIELD EQUATIONS AND SIMILARITY SOLUTIONS

Let us consider the metric of a spherically symmetric space–time, written in double-null coordinates[7]

$$ds^2=2f(u,v)du\ dv-R^2(u,v)(d\theta^2+\sin^2\theta\ d\varphi^2) \tag{1}$$

and the energy-momentum tensor corresponding to ingoing and outgoing null fluids

$$T_{\mu\nu}=\rho_1 l_\mu l_\nu+\rho_2 n_\mu n_\nu, \tag{2}$$

where $l_\mu=\delta^u_\mu$ and $n_\mu=\delta^v_\mu$. We usually assume that $\rho_1$, $\rho_2\geq 0$; more generally, if $\rho_1$ and $\rho_2$ are both of the same sign, this tensor can also be interpreted as representing an anisotropic fluid with pressure along the radial direction only;[8] the radial pressure equals the density $\rho=\sqrt{\rho_1\rho_2}$, and the four-velocity is given by

$$U_\mu=\left(\frac{\rho_2}{4\rho_1}\right)^{1/4}\left[n_\mu+\left(\frac{\rho_1}{\rho_2}\right)^{1/2}l_\mu\right]. \tag{3}$$

The Einstein equations for the metric (1) and the energy-momentum tensor (2) reduce to

$$h_{,uv}+f=0, \tag{4}$$

$$\left(\frac{f_{,u}}{f}\right)_{,v}=\frac{h_{,u}h_{,v}}{2h^2}+\frac{f}{h}, \tag{5}$$

$$\rho_1=-\frac{f}{\sqrt{h}}\left(\frac{h_{,u}}{\sqrt{h}f}\right)_{,u}, \tag{6}$$

$$\rho_2=-\frac{f}{\sqrt{h}}\left(\frac{h_{,v}}{\sqrt{h}f}\right)_{,v}, \tag{7}$$

where $h=R^2$. Since Eqs. (4) and (5) do not involve $\rho_1$ and $\rho_2$, we may solve them for the metric functions, and then calculate the densities using Eqs. (6) and (7).



This article is copyrighted as indicated in the article. Reuse of AIP content is subject to the terms at: http://scitation.aip.org/termsconditions. Downloaded to IP: 143.106.108.182 On: Mon, 22 Jun 2015 16:58:31

It can be shown that the general Lie point symmetry[9] of the system (4)–(5) is described by an infinitesimal generator of the form

$$\mathbf{X}=a\left(f\frac{\partial}{\partial f}+h\frac{\partial}{\partial h}\right)+\eta(u)\frac{\partial}{\partial u}+\xi(v)\frac{\partial}{\partial v}-[\eta'(u)+\xi'(v)]f\frac{\partial}{\partial f}, \tag{8}$$

where $a$ is an arbitrary constant, and $\xi$, $\eta$ are arbitrary functions of the indicated arguments; the prime, as usual, denotes differentiation with respect to the argument. To find Eq. (8), it is convenient to use a computer algebra program such as symmetries of partial differential equations (SPDE).[10]

Solutions of Eqs. (4)–(5) which are invariant under the finite transformation generated by Eq. (8) are known as *similarity solutions*.[9] These solutions may be expressed as relations between *similarity variables*, which are solutions $\sigma(u,v,f,h)$ of the first-order partial differential equation

$$\mathbf{X}\sigma=0.$$

By solving the preceding equation by the method of characteristics, it can be verified that a set of three independent similarity variables for the generator (8) is

$$\sigma_1(u,v)=\int^u\frac{du}{\eta(u)}-\int^v\frac{dv}{\xi(v)}, \tag{9}$$

$$\sigma_2(u,v,f)=f\eta(u)\xi(v)e^{-\Gamma}, \tag{10}$$

$$\sigma_3(u,v,h)=he^{-\Gamma}, \tag{11}$$

where

$$\Gamma(u,v)=\frac{a}{2}\left(\int^u\frac{du}{\eta(u)}+\int^v\frac{dv}{\xi(v)}\right).$$

This choice of similarity variables is not unique, since any function $\sigma=\Phi(\sigma_1,\sigma_2,\sigma_3)$ is also a similarity variable. However, we shall see below that the above choice is especially convenient in the study of similarity solutions.

For a similarity solution, $\sigma_2$ and $\sigma_3$ are both functions of the single variable $\sigma_1$; in other words, the similarity solutions have the form

$$f=\frac{e^{\Gamma}}{\eta(u)\xi(v)}\phi(w), \tag{12}$$

$$h=e^{\Gamma}\psi(w), \tag{13}$$

where $w\equiv\sigma_1$ and $\phi$, $\psi$ are functions to be determined. Substituting Eqs. (12)–(13) in Eqs. (4)–(5), we obtain the pair of ordinary differential equations

$$\psi''-\lambda\psi=\phi, \tag{14}$$

$$\frac{\phi''}{\phi}=\left(\frac{\phi'}{\phi}\right)^2+\frac{1}{2}\left(\frac{\psi'}{\psi}\right)^2-\frac{\phi}{\psi}-\frac{1}{2}\lambda, \tag{15}$$

where $()'\equiv d/dw$ and $\lambda=\frac{1}{4}a^2\geq 0$. It is a remarkable fact that this system is autonomous [that is, $w$ does not appear explicitly in Eqs. (14)–(15)] and also that arbitrary functions $\xi$ and $\eta$ lead always to the same system of ordinary differential equations. This is a consequence of our particular choice of similarity variables. In general, if we take



This article is copyrighted as indicated in the article. Reuse of AIP content is subject to the terms at: http://scitation.aip.org/termsconditions. Downloaded to IP: 143.106.108.182 On: Mon, 22 Jun 2015 16:58:31

$$\tilde{\sigma}_1 = A_1(\sigma_1),$$

$$\tilde{\sigma}_2 = \sigma_2 A_2(\sigma_1),$$

$$\tilde{\sigma}_3 = \sigma_3 A_3(\sigma_1)$$

as similarity variables, with the $A_j$ arbitrary functions of $\sigma_1$, then Eqs. (4)–(5) will reduce to a nonautonomous system which will not be the same for different choices of $\xi$ and $\eta$.

The previous remarks do not imply that different choices of $\xi$ and $\eta$ lead to different families of similarity solutions. In fact, it is easy to verify from Eqs. (1), (12), and (13) that if $\eta_1$, $\xi_1$, and $\eta_2$, $\xi_2$ are two possible choices of $\eta$, $\xi$ (which do not change sign), then for a given solution $\phi$, $\psi$ of Eqs. (14)–(15) the corresponding similarity solutions may be obtained from one another by a change of null coordinates of the form $\bar{u} = \alpha(u)$, $\bar{v} = \beta(v)$. Thus, it is sufficient to study the similarity solutions for one particular choice of $\eta$, $\xi$.

The system (14)–(15) is invariant under the scaling transformation $(\phi, \psi) \to (\epsilon\phi, \epsilon\psi)$, whose infinitesimal generator (extended to first-order derivatives) is

$$\mathbf{Y} = \phi \frac{\partial}{\partial \phi} + \psi \frac{\partial}{\partial \psi} + \phi' \frac{\partial}{\partial \phi'} + \psi' \frac{\partial}{\partial \psi'}.$$

The order of the system (14)–(15) may therefore be reduced by one by choosing as new variables a set of four first-order differential invariants[9] of the Lie group generated by $\mathbf{Y}$, that is, solutions $\Omega(w, \phi, \psi, \phi', \psi')$ of $\mathbf{Y}\Omega = 0$. In the present case, a set of independent invariants is

$$w, \quad F = \phi/\psi, \quad G = \phi'/\phi, \quad H = \psi'/\psi. \tag{16}$$

Differentiating Eq. (16) with respect to $w$, and using Eqs. (14)–(15), we obtain a system of three first-order equations for $F$, $G$ and $H$

$$F' = F(G - H), \tag{17}$$

$$G' = \tfrac{1}{2}(H^2 - \lambda) - F, \tag{18}$$

$$H' = F - (H^2 - \lambda). \tag{19}$$

Even though the nonlinearity in this first-order system is quadratic, it is not of Riccati type.[11] Thus, it probably cannot be solved by quadratures starting from a particular solution. Apart from the symmetry of translation in $w$, which reflects the fact that the system is autonomous, we have not found any other Lie point symmetry. The use of this symmetry to reduce Eqs. (17)–(19) to a pair of first-order equations leads to a nonautonomous system, which is actually no easier to analyze than a three-dimensional autonomous system. For this reason, we prefer to discuss the similarity solutions in terms of the solutions of Eqs. (17)–(19). Having a solution of this system, we can recover the functions $\phi$ and $\psi$ by integrating Eq. (16)

$$\psi = \exp\left( \int^w H(w) dw \right), \quad \phi = F\psi. \tag{20}$$

The densities of the null fluids corresponding to the similarity solutions can be easily calculated using Eqs. (6)–(7), (12)–(15), and (16)

$$\rho_1 = \frac{\hat{\rho}_1(w)}{[\eta(u)]^2}, \tag{21}$$



This article is copyrighted as indicated in the article. Reuse of AIP content is subject to the terms at: http://scitation.aip.org/termsconditions. Downloaded to IP: 143.106.108.182 On: Mon, 22 Jun 2015 16:58:31

$$\rho_2=\frac{\hat{\rho}_2(w)}{[\xi(v)]^2}, \tag{22}$$

$$\hat{\rho}_1(w)=H\left(G+\frac{1}{2}H\right)-F-\frac{1}{2}\lambda+\frac{a}{2}G, \tag{23}$$

$$\hat{\rho}_2(w)=H\left(G+\frac{1}{2}H\right)-F-\frac{1}{2}\lambda-\frac{a}{2}G. \tag{24}$$

## III. STUDY OF THE AUTONOMOUS SYSTEM FOR *F*, *G*, AND *H*

In this section we shall describe the qualitative behavior of the solutions to Eqs. (17)–(19) for arbitrary initial conditions. We will restrict ourselves to the case $\lambda=1$, since for $\lambda>0$ the system can always be reduced to this case by the rescaling of variables $(F,G,H,w)\rightarrow(\lambda F,\sqrt{\lambda}G,\sqrt{\lambda}H,w/\sqrt{\lambda})$. In the limiting case $\lambda=a=0$, we have from Eqs. (23)–(24) that $\hat{\rho}_1=\hat{\rho}_2$. Without loss of generality, we may choose $\eta=\xi\equiv-1$, which implies that $\rho_1=\rho_2$. It is easy to verify that the corresponding metric has the form (1) with $f$ and $R$ functions of $w=v-u$ only; depending on the sign of $f$, the coordinate $w$ can be either spacelike (in which case the metric is static) or timelike (in which case the metric does not have a simple interpretation). Therefore, the similarity solutions with $\lambda=a=0$ do not describe interesting null fluid interactions, and will not be further considered here.

The system (17)–(19) with $\lambda=1$ has critical points at

$$F=0,\quad G=g_0,\quad H=\pm1,$$

where $g_0$ is an arbitrary constant. Thus, the critical points lie on two parallel lines in $(F,G,H)$ space. The planes $H=\pm1$ will play an important role in the interpretation of the similarity solutions. Linearizing the system about a generic critical point, we obtain

$$F'\sim(g_0\mp1)F,$$

$$\delta G'\sim\pm\delta H-F,$$

$$\delta H'\sim F\mp2\delta H,$$

where $\delta G=G-g_0$, $\delta H=H\mp1$. The linearized system can be easily solved; we find

$$F\sim f_0e^{(g_0\mp1)w}, \tag{25}$$

$$\delta G\sim-\frac{f_0g_0}{g_0^2-1}e^{(g_0\mp1)w}-\frac{1}{2}h_0e^{\mp2w}, \tag{26}$$

$$\delta H\sim\frac{f_0}{g_0\pm1}e^{(g_0\mp1)w}+h_0e^{\mp2w}, \tag{27}$$

where $f_0$, $h_0$ are arbitrary constants. From this we see that the critical points with $H=1$ have two stable invariant directions for $g_0<1$ and one stable and one unstable invariant direction for $g_0>1$. Therefore, solutions approaching the line $F=0$, $H=1$ for $G<1$ will generally tend asymptotically to that line as $w\rightarrow\infty$. On the other hand, for $G>1$ most of the solutions initially approaching the "critical line" will ultimately get away from it. Analogously, for critical points with $H=-1$, there are two unstable invariant directions if $g_0>-1$ and one stable and one unstable invariant direction



This article is copyrighted as indicated in the article. Reuse of AIP content is subject to the terms at: http://scitation.aip.org/termsconditions.
Downloaded to IP: 143.106.108.182 On: Mon, 22 Jun 2015 16:58:31

if $g_0<-1$. Solutions approaching this "critical line" for $G>-1$ will tend asymptotically to a critical point as $w \to -\infty$; solutions approaching $F=0$, $H=-1$ with $G<-1$ behave as in the case $F=0$, $H=1$, $G>1$.

Substituting the asymptotic form of $(F,G,H)$ near the critical points into Eqs. (23)–(24), it may be verified that a solution approaching $H=1$ asymptotically as $w \to \infty$ has $\hat{\rho}_1 \to$ const and $\hat{\rho}_2 \to 0$ (we assume that $a>0$). In the same way, solutions approaching $H=-1$ asymptotically as $w \to -\infty$ have $\hat{\rho}_1 \to 0$ and $\hat{\rho}_2 \to$ const. Thus, solutions of the above kind represent situations where the two null fluids are asymptotically unmixed in some region of space–time.

Before considering general initial conditions we shall study two particular families of solutions of Eqs. (17)–(19) which may be found analytically.

(1) *Zero-density solutions.* It is clear from Eqs. (21)–(24) that the condition $\rho_1=\rho_2=0$ is equivalent to

$$G=0, \quad F=\tfrac{1}{2}(H^2-1). \tag{28}$$

When these conditions hold, Eq. (18) is automatically satisfied, and Eqs. (17) and (19) become consistent with each other. Integrating Eq. (19), which becomes

$$H'=-\tfrac{1}{2}(H^2-1)$$

we obtain the solution

$$H=\frac{1-ke^{-w}}{1+ke^{-w}}, \tag{29}$$

where $k$ is an arbitrary constant. The solution for $F$ is then

$$F=-\frac{2ke^{-w}}{(1+ke^{-w})^2}. \tag{30}$$

For $k>0$, the above solution is defined for all $w$, and its trajectory connects the two critical points lying in the plane $G=0$. For $k<0$, the solution is defined for $w \neq \ln(-k)$; in this case, the solution corresponds to two trajectories, one ending at the critical point $F=G=0$, $H=1$ and the other starting at $F=G=0$, $H=-1$. For all values of $k$, the trajectories of the solutions of this family lie on the parabola (28), which is plotted in Fig. 1. These solutions are trivial, since they are flat solutions, i.e., Minkoswki space written in accelerated spherically symmetric null coordinates; we will come back to this point later.

(2) *Solutions lying in the plane $F=0$.* It is clear from Eq. (17) that solutions starting at the plane $F=0$ will remain always in this plane. For such solutions, Eqs. (18) and (19) reduce to

$$H'=-2G'=1-H^2,$$

which may be integrated as

$$H=\frac{1-ke^{-2w}}{1+ke^{-2w}}, \quad G=-\frac{1}{2}H+c,$$

where $k$, $c$ are arbitrary constants. Therefore, the trajectories of these solutions lie on a family of parallel straight lines in the plane $F=0$. Even though these solutions give us a degenerate metric (since $F=0$ implies $f=0$), they can be used to deduce that no solution crosses the plane $F=0$.

We studied numerically the solutions of Eqs. (17)–(19) which cross the plane $G=0$ for some value of $w$ (without loss of generality, we can take this value to be zero). For these solutions, we verified that $\hat{\rho}_1$ and $\hat{\rho}_2$ are always of the same sign. At $w=0$, we have $\hat{\rho}_1=\hat{\rho}_2=\frac{1}{2}(H^2-1)-F$.



This article is copyrighted as indicated in the article. Reuse of AIP content is subject to the terms at: http://scitation.aip.org/termsconditions.
Downloaded to IP: 143.106.108.182 On: Mon, 22 Jun 2015 16:58:31

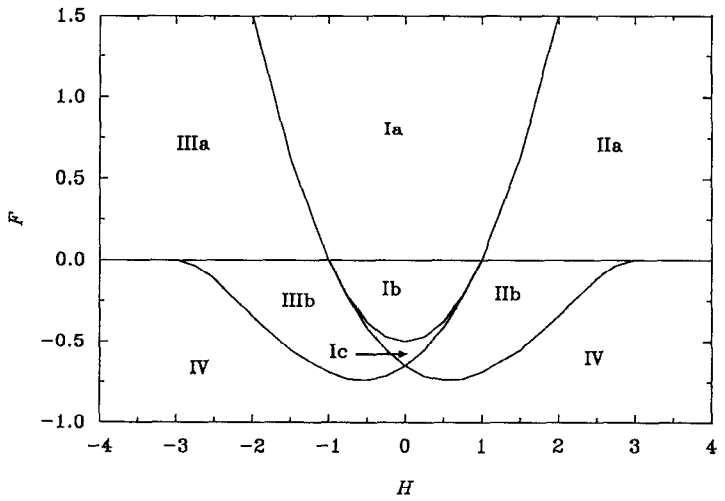


FIG. 1. The plane $G=0$ in $(F,G,H)$ space. Trajectories crossing this plane in each of the regions Ia, Ib, IIa, etc., have different qualitative behaviors (see text for more detail). The parabola $F=(1/2)(H^2-1)$ separates region Ib from Ic, and also Ia from IIa and IIIa. The other region boundaries have been determined by integrating Eqs. (17)–(19) numerically with different initial conditions on the $G=0$ plane.

Therefore, solutions crossing the plane $G=0$ at a point $(F_0,H_0)$ will have $\rho_1$, $\rho_2>0(<0)$ if $F_0<\frac{1}{2}(H_0^2-1)(F_0>\frac{1}{2}(H_0^2-1))$. The solutions which do not cross the plane $G=0$ seem to be less interesting, since our numerical study indicated that the relation $\hat{\rho}_1\hat{\rho}_2<0$ always holds in this case.

The behavior of the solutions which cross the plane $G=0$ depends on the intersection point $(F_0,H_0)$ in the following way (Fig. 1):

(1) If $(F_0,H_0)$ is in regions Ia, Ib, or Ic, the solution is defined for all $w$, and approaches a critical solution as $w\to\pm\infty$. The main difference among these solutions is that the ones corresponding to region Ia cross the planes $H=\pm1$ [Fig. 2(a)], while the ones corresponding to regions Ib and Ic do not [Fig. 2(b)].

(2) If $(F_0,H_0)$ is in regions IIa or IIb, the solution is defined in an interval of the form $w_{\min}<w<\infty$, and approaches a critical solution with $H=1$ as $w\to\infty$; the solution becomes singular ($F$, $G$, and $H$ diverge to infinity) as $w\to w_{\min}$. Solutions corresponding to region IIa have $F>0$, $H>1$ for all $w$ [Fig. 2(c)]. Solutions corresponding to region IIb have $F<0$, $H>-1$, and cross the plane $H=1$ exactly once [Fig. 2(d)].

(3) If $(F_0,H_0)$ is in region IIIa or IIIb (which are symmetric to regions IIa and IIb with respect to the $F$ axis), we can obtain the behavior of the solution by noting that Eqs. (17)–(19) are invariant under the transformation $(F,G,H,w)\to(F,-G,-H,-w)$ and using the results obtained for regions IIa and IIb. The solutions are defined in intervals of the form $-\infty<w<w_{\max}$ approaching a critical solution as $w\to-\infty$ and becoming singular as $w\to w_{\max}$.

(4) If $(F_0,H_0)$ is in region IV, the solution will be defined on a finite interval $w_{\min}<w<w_{\max}$, with singularities at both ends. The solution crosses both planes $H=\pm1$ at $w=w_-$ and $w=w_+$, respectively [Fig. 2(e)].

The behavior of the solutions near a singularity can be determined by the method of dominant balance;[12] the result is

$$F\sim c_1\delta^{-3/2}+c_1(\tfrac{2}{9}c_1^2\pm c_2)\delta^{-1/2}+O(1), \tag{31}$$

$$G\sim\mp\tfrac{1}{2}\delta^{-1}\pm\tfrac{2}{3}c_1\delta^{-1/2}+c_2+O(\delta^{1/2}), \tag{32}$$

This article is copyrighted as indicated in the article. Reuse of AIP content is subject to the terms at: http://scitation.aip.org/termsconditions. Downloaded to IP: 143.106.108.182 On: Mon, 22 Jun 2015 16:58:31

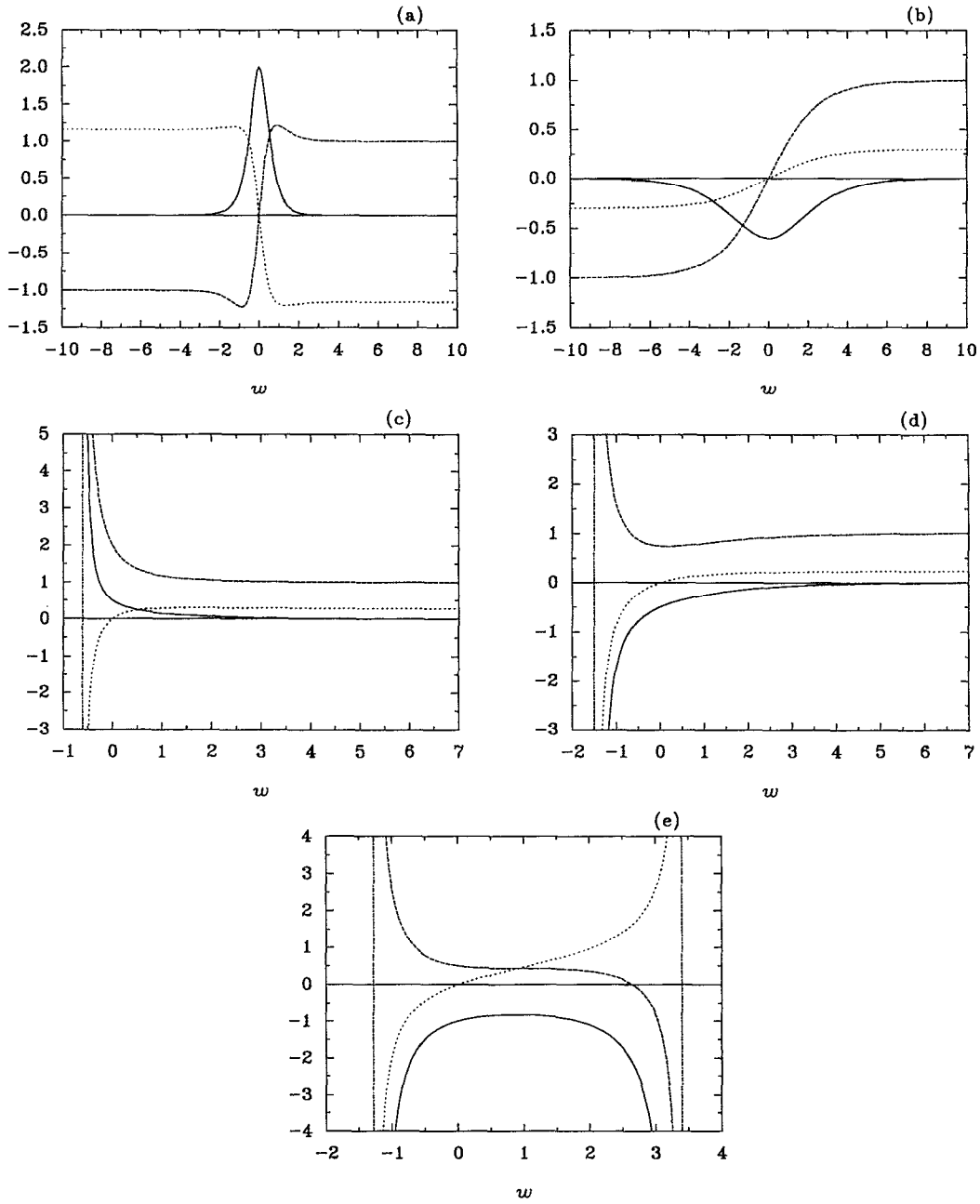


FIG. 2. Sample solutions which cross the plane $G=0$ in different regions: (a) Ia, (b) Ic (solutions in region Ib are similar to the ones in region Ic), (c) IIa, (d) IIb, (e) IV. Sample solutions for regions IIIa and IIIb may be obtained from (c) and (d) by using the symmetry property discussed in the text. The solid, dotted and dashed curves represent the similarity variables $F$, $G$, and $H$, respectively. In (c), (d), and (e), dash-dotted vertical lines indicate the values of $w$ where the solutions become singular.



This article is copyrighted as indicated in the article. Reuse of AIP content is subject to the terms at: http://scitation.aip.org/termsconditions. Downloaded to IP: 143.106.108.182 On: Mon, 22 Jun 2015 16:58:31

$$H\sim \pm\delta^{-1}\pm\tfrac{2}{3}c_1\delta^{-1/2}\mp\tfrac{2}{9}c_1^2+O(\delta^{1/2}), \tag{33}$$

where $\delta=\pm(w-w_0)\to 0$, $w_0$ can be either $w_{\min}$ (upper sign) or $w_{\max}$ (lower sign) and $c_1$, $c_2$ are arbitrary constants.

## IV. INTERPRETATION OF THE SOLUTIONS

As discussed in Sec. II, it is sufficient to study the similarity solutions for a particular choice of the arbitrary functions $\eta$, $\xi$. Here we choose

$$\eta=\epsilon_1\sqrt{1+u^2},\quad \xi=\epsilon_2\sqrt{1+v^2}, \tag{34}$$

where $\epsilon_j=\pm 1$; in this case, we have

$$w=\epsilon_1\sinh^{-1}u-\epsilon_2\sinh^{-1}v,$$

$$\Gamma=\epsilon_1\sinh^{-1}u+\epsilon_2\sinh^{-1}v.$$

The similarity solutions can describe the collision of two thick shells of null fluids traveling along opposite radial directions. For instance, if $\epsilon_1=\epsilon_2=1$ and $u\to-\infty$ with $v$ bounded, then $w\to-\infty$, so that for solutions which are defined in this limit we have $\hat{\rho}_1\to 0$, $\hat{\rho}_2\to$ const, (cf. Sec. III). Therefore, in this limit $\rho_2=\hat{\rho}_2/\xi^2\sim$const$/(1+v^2)$, which represents a thick shell of null fluid moving along the $u$ direction. Analogously, a thick shell of null fluid moving along the $v$ direction is obtained in the limit $v\to-\infty$ with $u$ bounded.

In the interpretation of the similarity solutions, it will be useful to analyze the behavior of the invariant built with the Riemann–Christoffel curvature tensor known as the Kretschmann scalar

$$K=R^{\alpha\beta\mu\nu}R_{\alpha\beta\mu\nu}$$

and of the "Coulomb" component of the Weyl tensor[7]

$$-\Psi_2\equiv\frac{1}{2}C^{\theta\varphi}_{\theta\varphi}=\frac{m(u,v)}{R^3}=\frac{1}{2R^2}\left(1+\frac{2R_{,u}R_{,v}}{f}\right), \tag{35}$$

which is the only independent component that does not vanish for spherical geometry. In this last relation, $m$ is called the mass parameter; for the Schwarschild solution, $m$ is the constant that represents the mass of the spherically symmetric center of gravitational attraction. For our similarity solutions, it can be shown by direct calculation that

$$R^4K=(4/F^2)[(H^2-1-2F)^2+GH(H^2-1-2F)+G^2(H^2-1)] \tag{36}$$

and

$$\frac{2m}{R}=1+\frac{(1-H^2)}{2F}; \tag{37}$$

note that $R^4K$ and $2m/R$ are functions only of the similarity parameter $w$. From these last two relations and Eq. (28) we have that the Kretschmann scalar and the mass function are both zero for the zero-density solutions. Then from the uniqueness of the Schwarzschild solutions[7] we conclude that the zero-density solutions are isometric to Minkowski space.

A marginally trapped surface is the locus of the points of zero expansion of an affine parameterized geodesic congruence of null rays;[6] these marginally trapped surfaces are also known as

This article is copyrighted as indicated in the article. Reuse of AIP content is subject to the terms at: http://scitation.aip.org/termsconditions.

Downloaded to IP: 143.106.108.182 On: Mon, 22 Jun 2015 16:58:31

apparent horizons. The null vectors $l^\mu$ and $n^\mu$ define two different congruences of null rays; since $l^\nu l^\mu{}_{;\nu}=n^\nu n^\mu{}_{;\nu}=0$, each null ray is an affine parameterized geodesic. The expansion of each geodesic is defined by

$$\theta(l)\equiv l^\mu{}_{;\mu}=\frac{2R_{,v}}{fR}, \quad \theta(n)\equiv n^\mu{}_{;\mu}=\frac{2R_{,u}}{fR}. \tag{38}$$

From Eqs. (35) and (38) we get

$$\frac{2m}{R}=1+\frac{1}{2}fR^2\theta(l)\theta(n). \tag{39}$$

Therefore, from this last equation and Eq. (37) we have that the apparent horizon condition, $\theta(l)\theta(n)=0$, is equivalent to $H^2=1$; any hypersurface $w=w_\mp$ such that $H(w_\mp)=\pm 1$ will be an apparent horizon.

In the rest of this section, we study the space–time and the density distributions corresponding to the different types of solutions presented in Sec. III, taking $\xi$ and $\eta$ as in Eq. (34). As we have seen, the solutions for $(F,G,H)$ may be classified according to the region of the plane $G=0$ which their trajectory intercepts (Fig. 1).

*Region Ia.* In this case, we always have $\rho_1$, $\rho_2<0$ (see Sec. III), so that we must interpret the energy-momentum tensor in terms of an anisotropic fluid (Sec. II). Since $F>0$, Eqs. (12) and (20) imply that $f$ and $\xi\eta$ have the same sign. Without loss of generality, we choose $\epsilon_1=\epsilon_2=1$ in Eq. (34), which implies that $f$ is positive and $w$ is a spacelike coordinate. Spacelike infinity then corresponds to the limit $w\to\infty$ with $\Gamma$ bounded; in this limit, we have verified numerically that the constants $f_0$, $g_0$, and $h_0$ appearing in Eqs. (25)–(27) satisfy the inequalities

$$f_0>0, \quad g_0<0, \quad h_0>0.$$

If $-1<g_0<0$, we may deduce from Eqs. (37), (25), and (27) that

$$m\sim\frac{g_0R}{2(g_0+1)}\to-\infty$$

so that the similarity solution does not have a simple interpretation; if $g_0<-1$, we can likewise deduce that

$$m\sim-\frac{h_0R}{2f_0}e^{-(1+g_0)w}\to-\infty$$

and again the solutions are not of great interest.

*Region Ib.* As in the previous case, we have $\rho_1$, $\rho_2<0$, so that we interpret the solution in terms of an anisotropic fluid. Since $F<0$, in order to have $f>0$ we must choose $\eta\xi<0$; taking $\epsilon_1=1$, $\epsilon_2=-1$, $w$ becomes a timelike coordinate. In this case, one may go to spacelike infinity through the limit $R\to\infty$ with $w$ constant. We have verified numerically that for this kind of solution the right hand side of Eq. (37) is negative for all $w$, so that again the solutions have an infinite negative mass function.

*Region Ic.* The space–time for this case is qualitatively similar to that of the previous case, but now $\rho_1$, $\rho_2>0$, so that we can interpret the solution in terms of two null fluids. The asymptotic behavior of $m$ is given by $m\sim k(w)R$ for $R\to\infty$ at constant $w$, where $k(w)$ is a positive function of $w$ [the positivity of $k(w)$ has been verified numerically]. This corresponds to densities which decay as $R^{-2}$ for large $R$. The solution (Fig. 3) represents an initially expanding shell of null fluid with density $\rho_2$ which is rapidly backscattered as a contracting null fluid of density $\rho_1$. Even



This article is copyrighted as indicated in the article. Reuse of AIP content is subject to the terms at: http://scitation.aip.org/termsconditions.
Downloaded to IP: 143.106.108.182 On: Mon, 22 Jun 2015 16:58:31

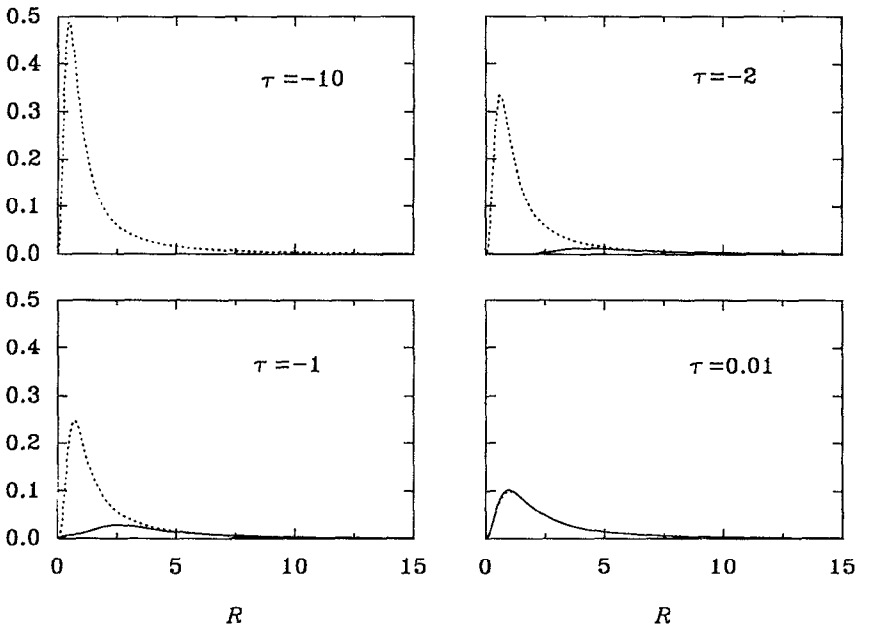


FIG. 3. Evolution of the null fluid densities for the solution shown in Fig. 2(b) (corresponding to region Ic). The timelike coordinate employed is $\tau=(u+v)/\sqrt{2}$. We have an initially expanding ($\tau=-10$) shell of density $\rho_2$ (dotted line) which is rapidly backscattered as a contracting shell of density $\rho_1$ (full line). Since the corresponding trajectory in $(F,G,H)$ space crosses the plane $G=0$ at the line $H=G=0$ [see Fig. 2(b)], it follows from the reflection symmetry mentioned in Sec. III that the evolution for $\tau>0$ is just the reverse of the evolution for $\tau<0$, with the ingoing and outgoing null fluid densities interchanged. For a general trajectory which crosses the $G=0$ plane in region Ic of Fig. 1, the evolution is qualitatively similar, although not perfectly symmetrical.

though the null fluid densities vanish at the center (Fig. 3), there is a singularity at $R=0$, since from Eq. (36) the Kretschmann scalar behaves as $K=O(R^{-4})$ as $R\to 0$ with $w$ fixed. We observe that this singularity is weaker than the Schwarschild singularity, which has $K=O(R^{-6})$,[13] and that it is present at all times. Thus, in contrast to the self-focusing singularities found in a previous study of the collision of cylindrical null fluids,[3] the singularity considered here simply supplies a background gravitational field in which the expanding null shell is backscattered. For this kind of solution $H^2<1$ and $F<0$ for all $w$, so that $R>2m$ everywhere and we do not have apparent horizons.

*Region IIa.* Solutions of this type have $\rho_1$, $\rho_2>0$ (Sec. III), and may therefore be interpreted in terms of two null fluids. Since $F>0$, we take $\epsilon_1=\epsilon_2=1$ in order to have $f>0$; $w$ will be a spacelike coordinate. As discussed in Sec. III, there is a singularity at $w=w_{\min}$; since here we have $H>1$ and $F>0$ for all $w>w_{\min}$, it follows from Eq. (37) that $R>2m$ everywhere and there is no apparent horizon (this is a naked singularity). Since near the singularity $H\sim\delta^{-1}$, where $\delta=w-w_{\min}$, it follows from Eq. (20) that $\psi=O(\delta)$ as $\delta\to 0$. Hence, from Eq. (13), $R=O(\delta^{1/2})$, which vanishes at $\delta=0$. Inserting Eqs. (31)–(33) into Eqs. (23)–(24) and (36), we can show that near the singularity the densities and the Kretschmann scalar behave as

$$\hat{\rho}_{1,2}\sim(c_2+\tfrac{5}{9}c_1^2\mp\tfrac{1}{2})\delta^{-1}=O(R^{-2}),$$

$$K\sim 3/c_1^2\delta R^4=O(R^{-6}).$$

The solution (Fig. 4) represents an ingoing null fluid layer which meets an expanding "core" of null fluid; at large times, a more detailed asymptotic analysis shows that the densities at any fixed

This article is copyrighted as indicated in the article. Reuse of AIP content is subject to the terms at: http://scitation.aip.org/termsconditions. Downloaded to IP: 143.106.108.182 On: Mon, 22 Jun 2015 16:58:31

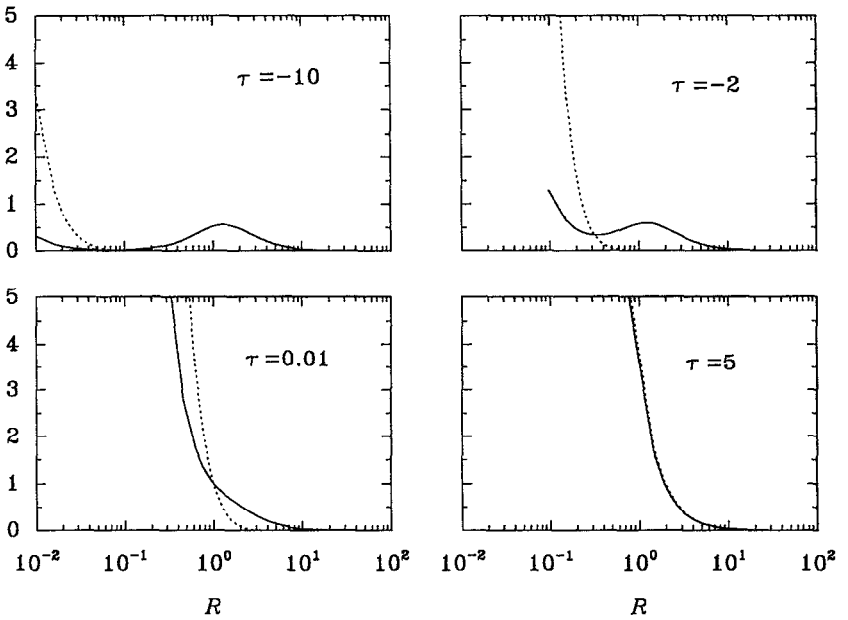


FIG. 4. Evolution of the ingoing (solid lines) and outgoing (dashed lines) null fluid densities for the solution shown in Fig. 2(c) (corresponding to region IIa). The timelike coordinate employed is $\tau=(u+v)/\sqrt{2}$. The initial configuration has an ingoing shell which meets an expanding "core" of null fluid. At later times, the ingoing and outgoing densities at each fixed radius $R=R_0$ approach constant values, and an equilibrium situation is reached. Even though the densities shown here seem to become equal as $\tau\to\infty$, it can be shown that in the limit of large times the density distributions are such that $\rho_1/\rho_2\to k$, where $k$ is a constant whose value depends on the chosen similarity solution.

radius $R=R_0$ approach constant values. At spacelike infinity, which corresponds to $w\to\infty$ with $\Gamma$ constant, we have verified numerically that the arbitrary constants in Eqs. (25)–(27) satisfy

$$f_0>0, \quad 0<g_0<1;$$

this implies that

$$m\sim\frac{g_0R}{2(g_0+1)}$$

so that the mass function is again positive but infinite.

*Region IIb.* Solutions of this type can again be interpreted in terms of two null fluids (Sec. III). Since $F<0$, in order to have $f>0$ we take $\eta\xi<0$; choosing $\epsilon_1=1$, $\epsilon_2=-1$, the coordinate $w$ becomes timelike. As discussed in Sec. III, there is a singularity at $w=w_{\min}$; as in the preceding case, this singularity also corresponds to $R=0$. Therefore, we have a cosmological model of the Kantowski–Sachs class with a Big Bang at $w=w_{\min}$ and an apparent horizon at a hypersurface $w=w_-$ such that $H(w_-)=1$ [Fig. 2(d)]. The behavior of the fluid densities for $w>w_{\min}$ is qualitatively similar to that of region Ic solutions, with an initially outgoing shell which is eventually backscattered.

*Region IIIa.* Due to the symmetry between regions IIa and IIIa (Sec. III), the interpretations of the corresponding solutions are very similar; the main difference is that $\rho_1$ and $\rho_2$ exchange roles and the sense of time is reversed. Thus, initially we have monotonic distributions of both $\rho_1$ and $\rho_2$ which later evolve into a collapsing core and an expanding shell.


This article is copyrighted as indicated in the article. Reuse of AIP content is subject to the terms at: http://scitation.aip.org/termsconditions. Downloaded to IP: 143.106.108.182 On: Mon, 22 Jun 2015 16:58:31

*Region IIIb.* Again by symmetry, solutions of this type can be interpreted in terms of those corresponding to region IIb by exchanging $\rho_1$ and $\rho_2$ and reversing the sense of time. We have an initially outgoing null fluid shell which is rapidly backscattered. The interaction of the ingoing and outgoing null fluids leads to the formation of an apparent horizon at a hypersurface $w=w_+$ such that $H(w_+)=-1$ and of a singularity at a later time $w=w_{\max}$, which again corresponds to $R=0$; for $R \to 0$, the Kretschmann scalar and the densities of the null fluids also behave as in region Ic. This case may also be interpreted as a Kantowski–Sachs cosmological model that ends in a Big Crunch.

*Region IV.* Since $F<0$, we take $\epsilon_1=1$, $\epsilon_2=-1$; $w$ will be a timelike coordinate. As we have seen in Sec. III, there are two singularities (at $w=w_{\min}$ and $w=w_{\max}$). Thus, in this case, we have also a cosmological model of Kantowski–Sachs type, but which now begins in a Big Bang and ends in a Big Crunch. These two singularities are clothed by apparent horizons at $w=w_-$ and $w=w_+$, respectively, where $H(w_\mp)=\pm 1$ [Fig. 2(e)]. Between the initial and final singularities, the behavior of the null fluid densities is qualitatively similar to that of region Ic solutions.

## V. CONCLUSION

We have studied in detail the similarity solutions of the Einstein equations representing two interacting spherical null fluids. Although some of these solutions may display certain undesirable features, such as infinite mass parameters at spacelike infinity and a naked singularity at $R=0$ which is present for all time, they constitute simple illustrations of certain physical processes which may occur in more realistic situations where two null fluids interact. These processes include backscattering (regions Ic and IIIb), the approach to an equilibrium situation (region IIa), and the formation of a new singularity as a result of the interaction between the null fluids (regions IIIb, IV). This last process has also been observed in an analytical model of the interaction of cylindrical null fluids[3] and is the basis of the mass inflation phenomenon.[4] Also, we have families of solutions that can be interpreted as cosmological models of the Kantowski–Sachs class with Big Bang, and sometimes also Big Crunch singularities.

A possible application for the similarity solutions presented here is the testing of numerical codes for the solution of Eqs. (4)–(7).

## ACKNOWLEDGMENTS

P. R. H. and A. W. wish to thank the hospitality of the Departamento de Matemática Aplicada of IMECC-UNICAMP wherein this work was initiated.

P. R. H. has been supported by Fundação de Amparo à Pesquisa do Estado de São Paulo (São Paulo, Brazil) under Grant Nos. 90/2834-2 and 93/5008-4.

[1] E. Schrodinger, *Expanding Universes* (Cambridge University, Cambridge, England, 1956).
[2] P. S. Letelier and A. Wang, Phys. Lett. A **182**, 220 (1993).
[3] P. S. Letelier and A. Wang, Phys. Rev. D **49**, 5105 (1994).
[4] E. Poisson and W. Israel, Phys. Rev. D **41**, 1796 (1990).
[5] R. Kantowski and R. K. Sachs, J. Math. Phys. **7**, 443 (1966).
[6] S. W. Hawking and G. F. R. Ellis, *The Large Scale Structure of Space–Time* (Cambridge University, Cambridge, England, 1973).
[7] S. Chandrasekhar, *The Mathematical Theory of Black Holes* (Oxford University, Oxford, 1992).
[8] P. S. Letelier, Phys. Rev. D **22**, 807 (1980).
[9] G. W. Bluman and J. D. Cole, *Similarity Methods for Differential Equations* (Springer, New York, 1974).
[10] F. Schwartz, SIAM Rev. **30**, 450 (1988).
[11] W. T. Reid, *Riccati Differential Equations* (Academic, New York, 1972).
[12] C. M. Bender and S. A. Orszag, *Advanced Mathematical Methods for Scientists and Engineers* (McGraw-Hill, New York, 1978).
[13] B. Waugh and K. Lake, Phys. Rev. D **34**, 2978 (1986).



This article is copyrighted as indicated in the article. Reuse of AIP content is subject to the terms at: http://scitation.aip.org/termsconditions.
Downloaded to IP: 143.106.108.182 On: Mon, 22 Jun 2015 16:58:31